3D printed polymers are less stable than injection moulded counterparts when exposed to terminal sterilization processes using novel vaporized hydrogen peroxide and electron beam processes

Yuanyuan Chen[1], Martin Neff[5], Brian McEvoy[4], Zhi Cao[3], Romina Pezzoli[2], Alan Murphy[3], Noel Gately[2], Michael Hopkins Jnr[2], Neil J. Rowan[6], Declan M. Devine[1]

[1] *Materials Research Institute, Athlone Institute of Technology, Ireland*
[2] *Applied Polymer Technology (APT), Athlone Institute of Technology, Ireland*
[3] *Centre for Industrial Service & Design (CISD), Athlone Institute of Technology, Ireland*
[4] *STERIS Applied Sterilization Technologies (AST), Tullamore, Co. Offaly, Ireland*
[5] *ARBURG Plastic Freeforming (APF), Arburg GmBh & Co KG, Lossburg, Germany*
[6] *Centre for Disinfection, Sterilization and Biosecurity (CDSB), Athlone Institute of Technology, Ireland*

Keywords:
Sterilization, VHP, E-beam, 3D printing, injection moulded, high density polyethylene, polyamide 6

ABSTRACT

There is an increasing trend for use of 3D printing processes in healthcare due in part to emergence of customised medical devices and associated low manufacturing cost. However, there is a dearth of knowledge on the efficacy of terminal sterilization processes on such 3D printing processes compared to conventional manufacturing methods, such as injection moulding. Therefore, the goal of this timely work was to compare the mechanical, thermal and chemical effects of vaporized hydrogen peroxide (VHP) and electron beam (E-beam) sterilization processes on the 3D printed and injection moulded high density polyethylene (HDPE) and Polyamide 6 samples. Characterization of materials post sterilization was performed by several analytical methods. Studies found that injection moulded samples exhibited higher tensile strength, higher degree of crystallinity, lower ductility, and higher thermal stability than 3D printed samples due to their tightly packed structures. After VHP and E-beam sterilization processes, oxidation and crosslinking occurred along with yellow colour change. Free hydroxyl radicals and intermolecular carbon bonding were detected by FTIR; the viscosity, storage modulus and loss modulus were increased due to crosslinking; the wettability of all the samples were increased due to the free radicals on the surface. However, the tensile properties of all samples measured were not affected by the VHP or E-beam processes, which was attributed to the low irradiation dosage of E-beam and good resistance to hydrolytic degradation from VHP. Overall, E-beam process resulted in more severe oxidation and crosslinking than VHP process, and sterilized 3D printed samples were less stable compared to injection moulded samples when exposed to terminal sterilization processes, which was evidenced with more new peaks related to oxidation and crosslinking detected by FTIR and the dramatic increase in the degree of crystallinity. These findings highlight the importance of considering choice of industrial terminal sterilisation with view to future reduction of processing conditions for emerging additive manufacturing processes, such as in situ 3D printing that is often underappreciated.

Corresponding author: yuanyuanchen@ait.ie; Tel.: +353 90 6483047

INTRODUCTION

3D printing is a disruptive technology that is revolutionizing the healthcare industry globally. It enables custom-tailored medical devices to be printed to meet personalized needs, expedites surgical procedures, prepares surgeons and physicians with models for some complex cases, reduces the manufacturing cost, and may in time be used to replace human organ transplants in regenerative tissue engineering [1]. Currently, many medical devices are manufactured via 3D printing technology, such as hearing aids, orthopaedic and cranial implants, dental crowns and external prosthetics. As the majority of medical devices require sterilization, the performance of 3D printed devices finished with sterilization compared with traditionally manufactured devices is an important aspect to be considered as the healthcare manufacturing industry seeks to innovate with the 3D printing technology. The findings from this study provided evidence and support for the improvement of the sterilization procedures and standards servicing the fast development of 3D printed medical device industry.

Sterilization is a process by which bacteria or other living microorganisms are either destroyed or completely removed from a treated object [2]. Sterilization methods can be classified into three major groups namely, ionising radiation, gas technologies and heat treatment (steam). Ionising radiation includes gamma radiation, electron beam (E-beam) and X-ray radiation. Gas sterilization technologies comprise plasma, ethylene oxide (EO) and more recently, vaporized hydrogen peroxide (VHP®, a registered trademark of STERIS) [3]. Approximately 50% of medical devices are sterilized by using EO globally [4]. In response to the February 2019 closure of a large device sterilization facility, the FDA announced an innovative challenge to reduce the ethylene oxide emission [5], STERIS Applied Sterilization Technologies have investigated material compatibility with traditional terminal sterilization technologies and VHP appeared to be an alternative sterilization technology to EO. Steam sterilization is typically conducted by use of autoclaves and contrasts from aforementioned processes as relies upon heat for efficacy. This current work focuses on VHP and E-beam sterilization processes.

VHP is a gaseous technology, utilizing hydrogen peroxide (H_2O_2) in the form of vapour. H_2O_2 is an extremely powerful oxidant and it generates reactive oxygen species, such as hydroxyl radicals that attack multiple molecular targets, including microbial nucleic acids, enzymes, cell wall proteins and lipids. Typical VHP processes operate at a temperature range of 25 – 50 °C with an approximate cycle duration of 1.5 – 4 hours, but has limited penetration power [6]. It is suitable for materials that cannot sustain high temperature and moisture from steam sterilization, but it is not suitable for hygroscopic materials that absorb moisture, such as paper, cotton, cellulose, polylactic acid. [1, 2]. VHP is not classed as a carcinogen and is more environmentally friendly than EO as a sustainable terminal sterilization technology for medical device industry [8].

E-beam radiation is created by the accelerated electrons produced from an electromagnetic filed in an accelerator and the high-energy electrons move through the target material, killing bacteria by breaking the chains of DNA and RNA. However, this process can also lead to significant alternations in the treated materials. The high-energy electrons interact freely with molecules within the target material, ejecting electrons from their orbits and generating free radicals. The free radicals react with the present oxygen, lead to oxidation and degradation [2, 3]. The sterilization induced polymer degradation can be cross-linking, chain scission or a combination of both. Polymers with strong bonds such as benzene rings, might regain original configuration following sterilization, while polymers with weak bonds result in chain scission and undergo degradation [2, 9].

High density polyethylene (HDPE) in general crosslinks on irradiation, which increases the molecular weight and therefore lower the mobility of molecules and reduce creep. This may raise the tensile strength, increase the hardness and brittleness, but impact strength and shear strength usually decrease or remain relatively unchanged [12]. However, there is a chain

scission mechanism as well. It was reported that with 100 kGy radiation dosage, chain scission of HDPE occurred [13].

Polyamides are commonly known as nylon with repeating amide group along the polymer chain. Polyamides are limited to a few cycles of stream or autoclave sterilization because polyamides absorb moisture and hence degrade [14]. Polyamides are reasonably resistant to small doses of irradiation sterilization, typically up to 40 – 50 kGy, but not for many repeat doses [10, 12]. Kubyshkina *et al*. reported that polyamides are only suitable for a single dose of radiation [15]. Polyamides crosslink and lose crystallinity upon sterilization causing a slow increase in tensile strength but much more rapid drop in impact strength [12].

The effects of sterilization methods on various polymer materials have been studied, but there is a currently a dearth of evidence-based research describing the effects of industrial terminal sterilization processes on 3D printed plastic objects. Shaheen *et al*. printed tooth replicas**,** orthognathic splints and surgical cutting guides via PolyJet technology, and sterilized with autoclave (heat/steam sterilization) and VHP. They reported that all 3D printed objects that underwent autoclave and VHP sterilization had indicated shape deformation, and larger differences were observed with autoclave sterilization compared with VHP sterilization [16].

Unlike to conventional medical devices manufacturing techniques, such as machining and injection moulding, 3D printing is an additive method and the material is consequently added in each layer as a thin cross section of a 3D object. This layering process results in various changes in the physical, mechanical, thermal properties of the objects. Several studies have compared the property differences of polymers, including polycarbonate urethane [17], ABS [18], resulted from 3D printing and traditional manufacturing methods.

This current multi-disciplinary study characterises material properties of 3D printed and injection moulded Marlex (HDPE) and 3D printed Grilon (Polyamide 6) samples post terminal VHP and E-beam sterilization. The physical, chemical and thermal properties of the samples were investigated via colorimetry, rheometry, fourier transfer infrared spectroscopy (FTIR), dynamic mechanical thermal analysis (DMTA), differential scanning calorimetry (DSC), thermogravimetric analysis (TGA), and tensile testing. Surface modifications induced by sterilization were studied by scanning electron microscopy (SEM) and goniometry.

MATERIALS AND METHODS

Materials

High density polyethylene (HDPE) (Marlex® HHM 5502BN Polyethylene) was obtained from Chevron Philips Chemical Company LP (Woodlands, US). Polyamide 6 (Grilon F 40 NL) was supplied by EMS-CHEMIE AG (Switzerland). All materials were used as received.

Injection moulding

ASTM Standard tensile test samples were injection moulded by Arburg™ All-rounder 221K (Arburg, Lossburg, Germany), with the maximal clamping force of 350 kN, a screw diameter of 25 mm, a theoretical stroke volume of 49 cm^3 and a maximum injected part weight of 41 g. Marlex was dried at 70 °C for 8 hours prior to injection moulding. The temperature profile for injection moulding increased from 160 °C at the hopper to 200 °C at the nozzle with injection speed of 100 mm/s. The holding pressure used was 600 bar with a holding time of 6.5 seconds. The cooling time was 10 seconds with a back pressure of 50 bar. Polyamide 6 Grilon F 40 NL is an extrusion grade polymer and as such inaccurate geometries were obtained from injection moulding. Therefore, the comparison between 3D printed and injection moulded was conducted using Marlex samples only, with the comparative effects of VHP and E-beam on 3D printed parts assessed using both Marlex and Grilon samples.

3D printing

3D printed dumbbell-shaped tensile test samples were printed by ARBURG Plastic Freeforming (AKF) (ARBURG GmbH & CO KG, Germany). Marlex samples were printed at 200 °C and Grilon samples were printed at 250 °C. AKF allows molten plastic droplets with a

diameter between 0.2 and 0.4 mm to be generated by a stationary nozzle that relies on piezoelectric closure system and deposited on a moving platform to build up 3D objects layer by layer [19].

Vaporized hydrogen peroxide (VHP)

The test samples were treated with VHP in a STERIS VHP® LTS-V industrial sterilizer using STERIS VAPROX® hydrogen peroxide (35 %) sterilant. The process consisted of a four VHP pulse injection cycle performed in vacuum environment conditions at 30 °C. The process was performed at STERIS Applied Sterilization Technologies, Tullamore, Ireland.

E-beam

The test specimens were irradiated with E-beam process in STERIS with a Mevex Linac E-beam 10 MeV, 20 kW at a dose of circa 30 kGy in air at ambient temperature. All the specimens were irradiated by E-beam from both sides. The process was performed at STERIS Applied Sterilization Technologies, Tullamore, Ireland.

Colorimetry

Colour measurements (L*, a*, b* values) of the specimens was determined by using a Lovibond RT Series Reflectance Tintometer (Amesbury, UK) with OnColor software. Prior to measuring the colour of the specimens, the instrument was standardized by placing black and white standard plates and L*, a* and b* colour values were recorded. The L* values correspond to lightness/darkness (0 for black and 100 for white), the a* values correspond to the specimen's colour dimension from red to green (the greater a* value, the redder), the b* values correspond to the specimen's colour dimension from yellow to blue (the greater b* value, the yellower).

Surface wettability

The surface wettability of all the specimens was assessed using a First ten angstroms, FTA32 goniometer (Virginia, US). In this test, the Sessile Drop contact angle technique was utilised with distilled water as the probe liquid and the contact angle value of each specimen was recorded.

Fourier transfer infrared spectroscopy

Attenuated total reflectance Fourier transform infrared spectroscopy (FTIR) was carried out on a Perkin Elmer Spectrum One (Waltham, US) fitted with a universal ATR sampling accessory. All data were recorded at 21 ℃ in the spectral range of 4000 – 520 cm^{-1} against air as background, utilising a 4 scan per sample cycle at a resolution of 0.5 cm^{-1} and a fixed universal compression force of 70 - 80 N. Subsequent analysis was carried out using Spectrum software.

Differential scanning calorimetry

Differential scanning calorimetry (DSC) was carried out using a DSC 2920 Modulated DSC (TA Instruments, New Castle, US) with a nitrogen flow rate of 20 ml/min to prevent oxidation. Calibration of the instrument was performed using indium as standard. All the samples were dried at 60 °C for 8 hours prior to testing. Test specimens weighed between 8 and 12 mg were measured on a Sartorius scales (MC 210 P), capable of being read to five decimal places. Samples were crimped in non-perforated aluminium pans, with an empty crimped aluminium pan used as the reference. The thermal history of Marlex samples was removed by heating samples from 20 °C to 200 °C at the rate of 30 °C/min, and then held isothermally at 200 °C for 10 min. The samples were then cooled down from 200 °C to 0 °C at 30 °C/min. Finally, the thermal properties of the Marlex samples were recorded by heating the samples from 0 °C to 200 °C at the rate of 10 °C/min. Similarly, the Grilon samples were heated initially from 20 °C to 250 °C at the rate of 30 °C/min, then held isothermally at 250 °C for 10 min, followed by cooling down from 250 °C to 0 °C at 30 °C/min. Finally, the Grilon samples were heated again from 0 °C to 250 °C at the rate of 10 °C/min for testing thermal properties. Crystallinity and melting temperature of each sample were analysed. For calculating percentage crystallinity, the melt enthalpy of completely crystalline Marlex was 286.7 J/g and 83 J/g for Grilon.

Rheometry

An oscillatory rheometer TA Discovery Hybrid Rheometer 2 (New Castle, US) was used for the rheologic analysis of all the samples. The parallel plate rheometer was fitted and calibrated with a geometry of 25 mm diameter steel plate. An amplitude of 1 % was applied and previously verified by an amplitude sweep at a frequency of 1.0 Hz. Oscillation frequency sweeps were conducted from 0.1 to 20 rad/s angular frequency at a constant temperature of 260 °C for the Grilon samples and 250 °C for the Marlex samples.

Dynamic mechanical thermal analysis (DMTA)

The Dynamic mechanical thermal analysis (DMTA) analysis was carried out using Perkin Elmer DMA 8000 Analyser (Waltham, US) with Multi-Frequency module – Storage modulus and Strain. The heating profile for Marlex samples was from -150 to 10 °C at 3 °C/min, and the heating profile for Grilon samples was from -10 to 100 °C at 3 °C/min. The storage modulus and loss modulus of all samples were recorded.

Thermogravimetric analysis

Thermogravimetric analysis (TGA) tests were conducted using Perkin Elmer TGA 7 Thermogravimetric Analyzer (Waltham, US), coupled with a Perkin Elmer Thermal Analysis controller TAC7/DX under nitrogen atmosphere. The tests were run from 30 °C to 600 °C, at a heating rate of 10 °C/min. the onset degradation temperature of each sample was recorded.

Morphology

Scanning electron microscopy (SEM) was performed using a Mira XMU SEM (Tescan™, Czech Republic) in back scattered electron mode for surface analysis. The accelerating voltages utilized were 5 kV and 10 kV. Prior to analysis, test samples were placed on an aluminum stub, and the samples were sputtered with a gold using Baltec SCD 005 for 110 s at 0.1 mbar vacuum before testing.

Mechanical testing

The mechanical properties of the samples were characterised by tensile tests. Tensile testing was carried out on a Lloyd Lr10k tensometer (Ametek Ltd., West Sussex, UK) using a 2.5 kN load cell on ASTM standard test specimens at a strain rate of 5 mm/min for both 3D printed and injection moulded Marlex samples and 120 mm/min for Grilon samples. Data was recorded using Nexygen™ software. The tensile tests were carried out in adherence to ASTM D 882. Five replicates were analysed per group and prior to testing the thickness of each sample was measured. The percentage strain at maximum load and Young's Modulus of each sample were recorded.

Statistical analysis

Statistical analysis was performed using one way analysis of variance (ANOVA) with a Tukey Post hoc test to determine differences. Differences were considered significant when $p \leq 0.05$. The software used to perform statistical analysis was SPSS (IBM Version 22) for Windows. All data collected in this study were expressed as mean ± standard deviation. Sample size of 10 was used for colorimetry and contact angle test, while sample size of 5 was used for tensile testing.

RESULTS

Colorimetry

Both VHP and E-beam sterilization processes caused all the specimen turn yellow, and E-beam treated specimen appeared yellower than VHP treated specimen. This was supported by the colorimetric test results, where the b values and ΔE measurements increased dramatically, especially after E-beam treatment, shown in figure 1 and figure 2 ($p < 0.05$ for all comparison). The b values correspond to the colour of yellow, the greater b value, the yellower.

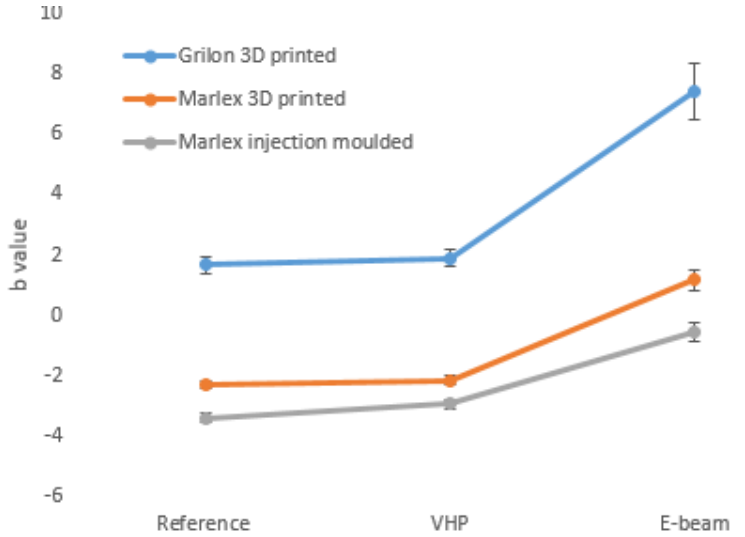

Figure 1: The b value from colorimetry for Marlex and Grilon samples

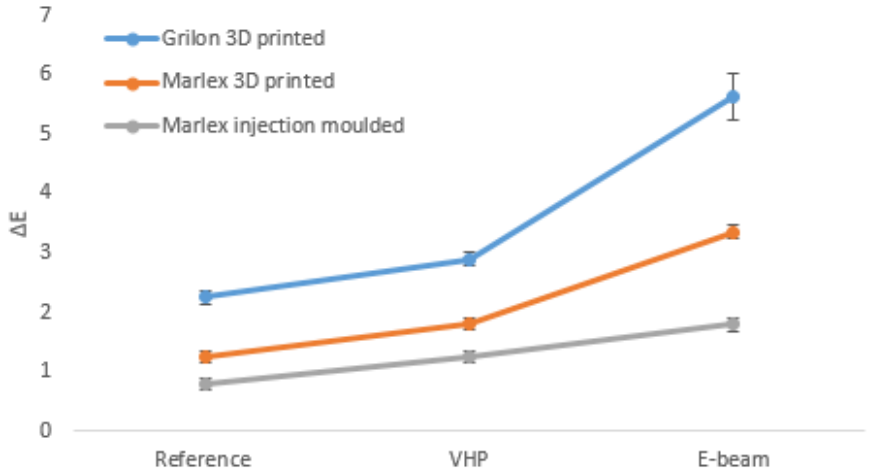

Figure 2: The ΔE from colorimetry for Marlex and Grilon samples

Surface wettability

Wettability is the tendency of a material to attract water to its surface, or absorb the water. Contact angle was measured to analyse the wettability of each sample. It can be clearly seen from figure 3 that VHP and E-beam sterilization methods decreased the contact angle of 3D printed Marlex samples, injection moulded Marlex samples and 3D printed Grilon samples ($p = 0.021$ for all comparison).

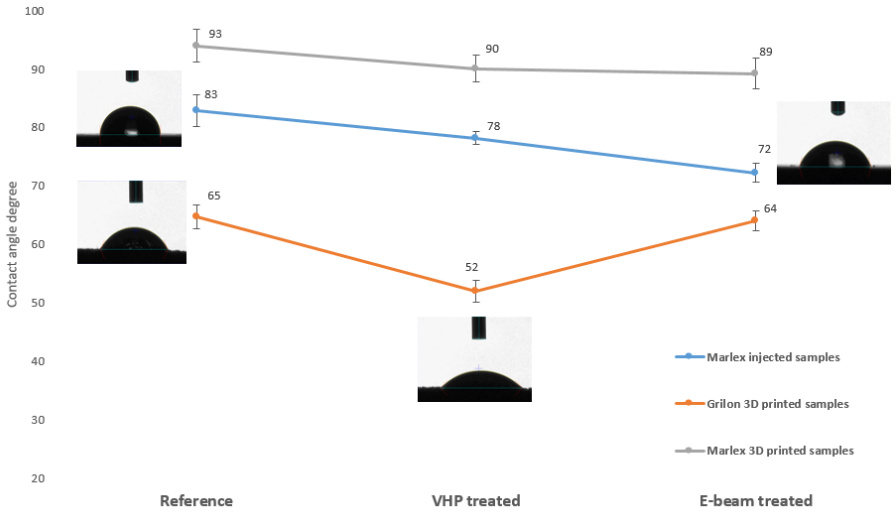

Figure 3: Contact angle measurements of 3D printed and injection moulded Marlex and Grilon samples upon VHP and E-beam sterilization

Fourier transfer infrared spectroscopy

A new peak at 3299 cm^{-1} , which is related to oxidation, appeared in the E-beam treated 3D printed Marlex sample; new peaks at 2022 and 2167 cm^{-1} related to C ≡ C bonding appeared in both E-beam and VHP treated 3D printed Marlex samples, and new peaks at 1541 and 1640 cm^{-1} asociated with C = C strech appeared in E-beam treated 3D printed Marlex samples, shown in figure 4. The mentioned new peaks at 3299, 2022 and 2167 cm^{-1} appeared in E-beam treated 3D printed Marlex samples, but not in the E-beam treated injection moulded Marlex samples, shown in figure 5. Figure 6 revealed the chemical bonding in Grilon samples upon VHP and E-beam processes and no great difference can be found.

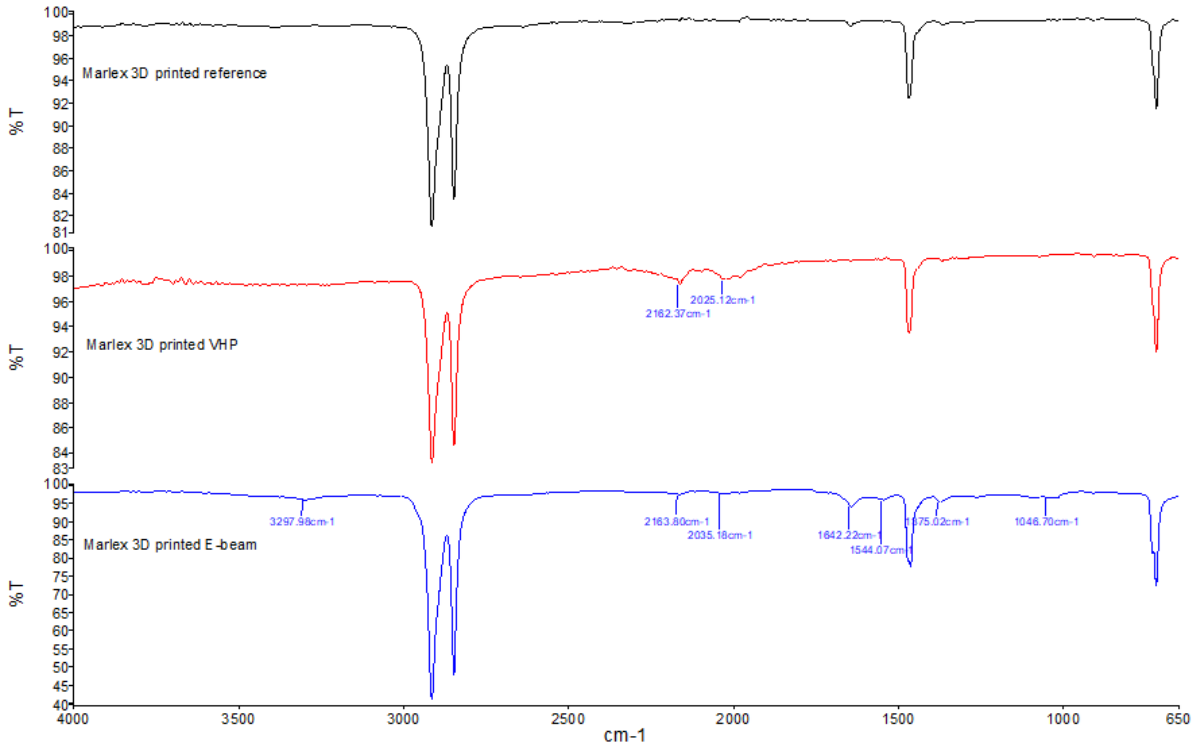

Figure 4: A: FTIR spectra of Marlex 3D printed samples

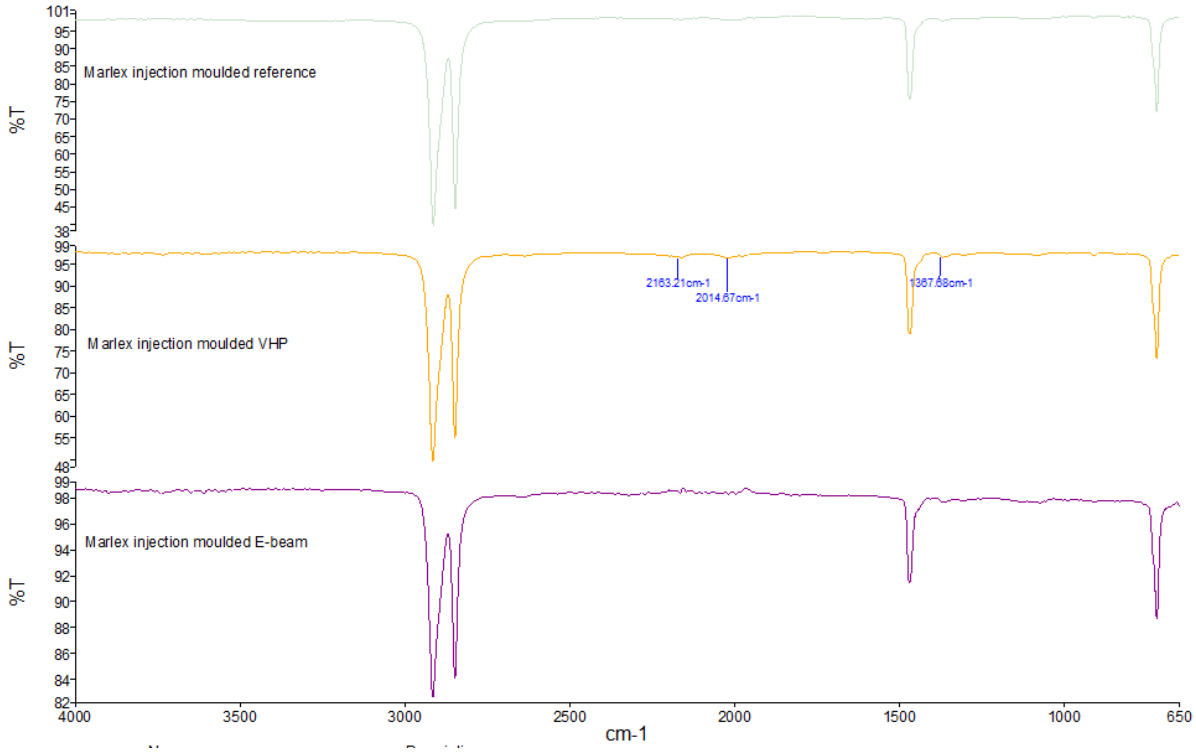

Figure 5: FTIR spectra of Marlex injection moulded samples

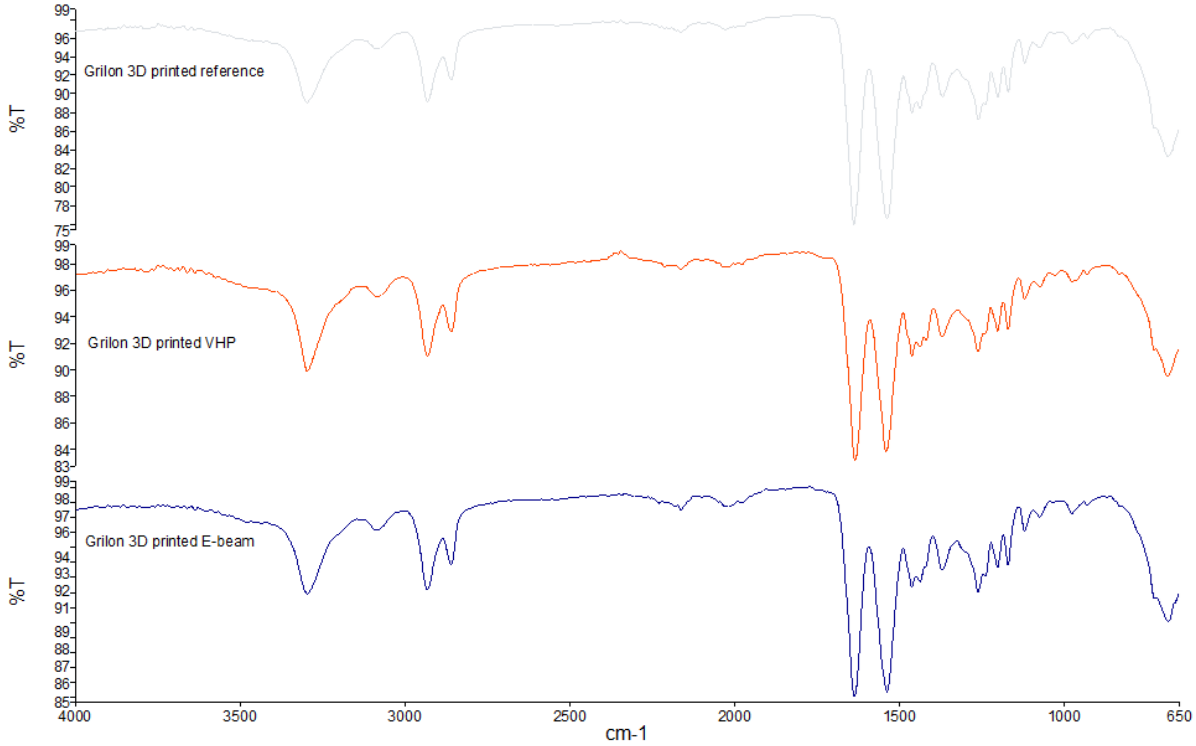

Figure 6: FTIR spectra of Grilon 3D printed samples

Differential scanning calorimetry

DSC was carried out to investigate the thermal characteristics of the test samples. VHP and E-beam processes did not change the T_m of any Marlex samples, but reduced the Tc of injection moulded Marlex samples from 111 °C of reference samples to 108 °C of VHP treated samples and 105 °C of E-beam treated samples, shown in table 1, figure 7 and 8. In addition, it was found that injection moulded Marlex samples had higher degree of crystallinity Xc (%) than 3D printed Marlex samples, and the VHP and E-beam processes increased the Xc of 3D printed Marlex samples from 64 % to 66 % and 83 % respectively, while the VHP and E-beam

processes did not cause a dramatic increase in the injection moulded Marlex samples with 79 % for pre-sterilization, 83 % after VHP treatment and 81 % after E-beam process. Figure 9 illustrated the DSC curves of the 3D printed Grilon samples. Similarly, the T_c and T_m of Grilon samples remained unchanged at 178 and 220°C respectively, and sterilization processes increased the percentage of crystallinity slightly, with 72% for reference, 78% for VHP treated and 76% for E-beam treated 3D printed Grilon samples.

Table 1: DSC results of 3D printed and injection moulded Marlex and Grilon samples upon VHP and E-beam sterilization

Samples	Tm	Tc	Xc %
Marlex 3D ref	135	109	64
Marlex 3D VHP	133	111	66
Marlex 3D E-beam	133	110	83
Marlex inject ref	135	111	79
Marlex inject VHP	134	108	83
Marlex inject E-beam	134	105	81
Grilon 3D ref	220	178	72
Grilon 3D VHP	222	178	78
Grilon 3D E-beam	221	176	76

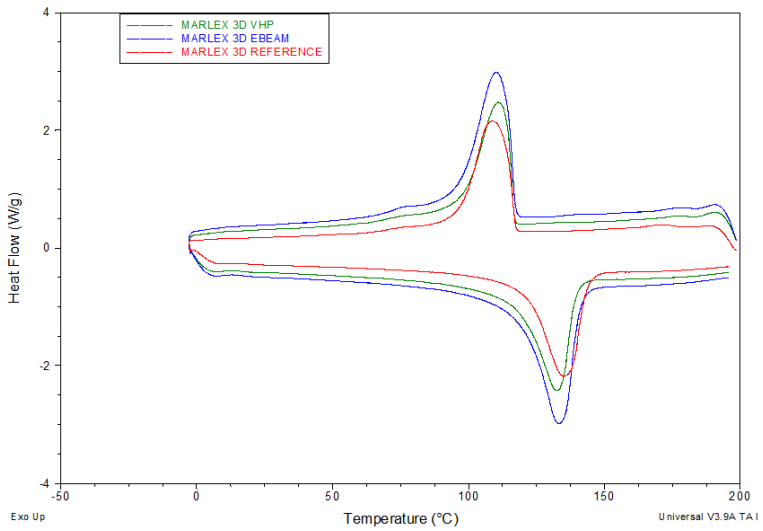

Figure 7: DSC curves of 3D printed Marlex samples

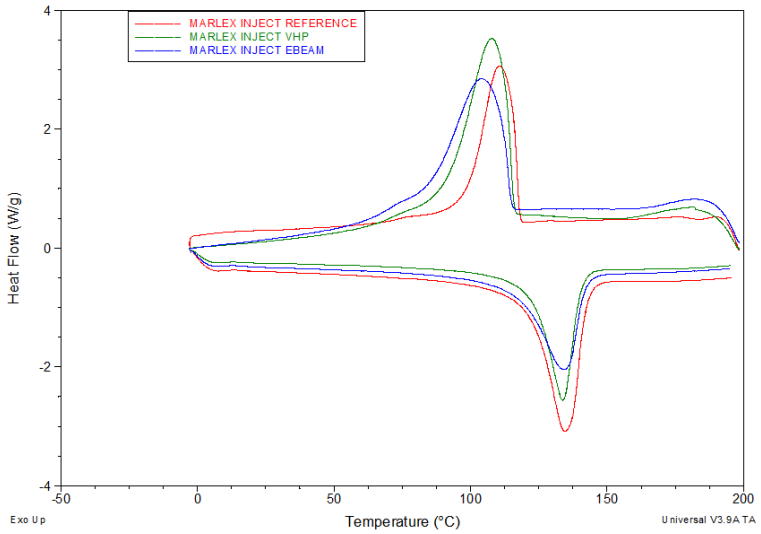

Figure 8: DSC curves of injection moulded Marlex samples

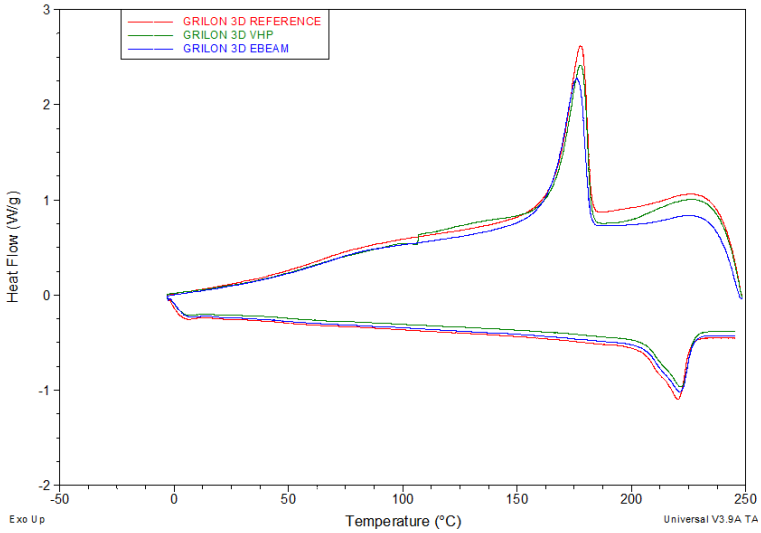

Figure 9: DSC curves of 3D printed Grilon samples

Rheometry & Dynamic mechanical thermal analysis

The plastic deformation of all the samples were analysed by rheometry and DMTA. The complex viscosity, storage modulus and loss modulus of both 3D printed and injection moulded Marlex and 3D printed Grilon samples increased on both VHP and E-beam sterilization processes. Compared to VHP, E-beam process resulted in higher complex viscosity, storage modulus and loss modulus in all three groups, shown in figure 10, 11 and 12.

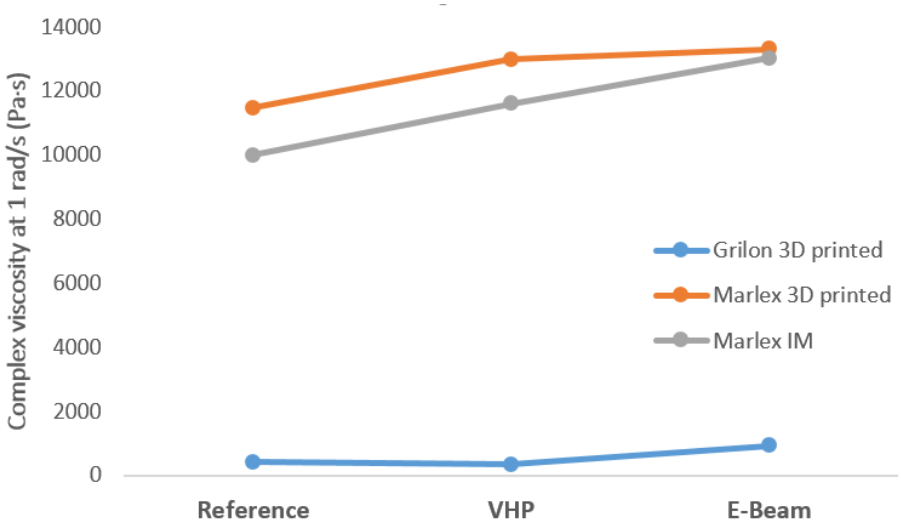

Figure 10: Complex viscosity of 3D printed and injection moulded Marlex samples and 3D printed Grilon samples

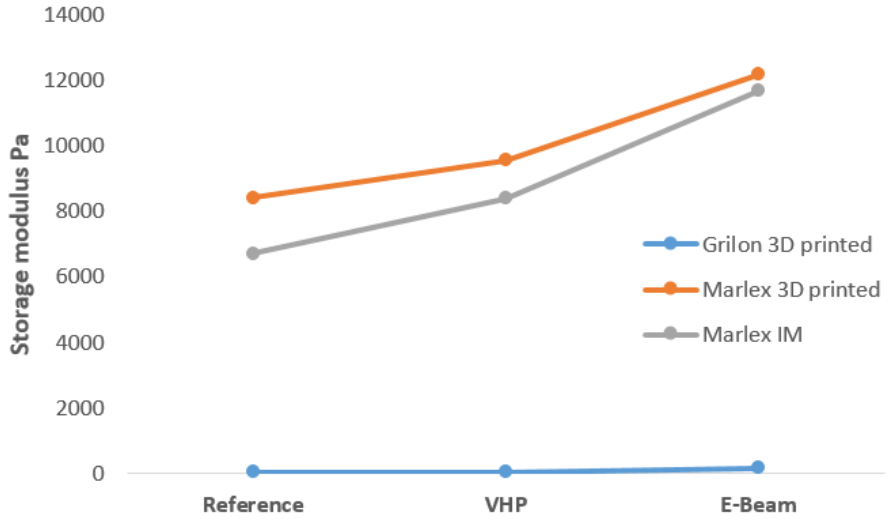

Figure 11: Storage modulus of 3D printed and injection moulded Marlex samples and 3D printed Grilon samples

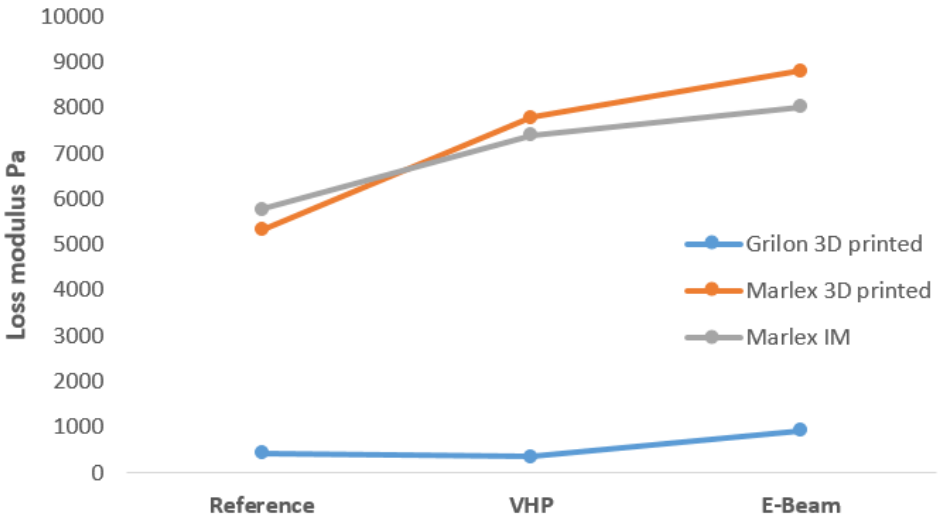

Figure 12: Loss modulus of 3D printed and injection moulded Marlex samples and 3D printed Grilon samples

Thermogravimetric analysis

The thermal stability of both 3D printed and injection moulded Marlex and 3D printed Grilon samples was evaluated by TGA. The degradation onset temperature of the injection moulded Marlex samples was 420 °C, which was higher than that of 3D printed Marlex samples (406

°C), shown in figure 13. VHP or E-beam processes did not affect the degradation onset temperature of injection moulded Marlex samples, 3D printed Marlex samples and 3D printed Grilon samples (447°C), shown in figure 13 and 14.

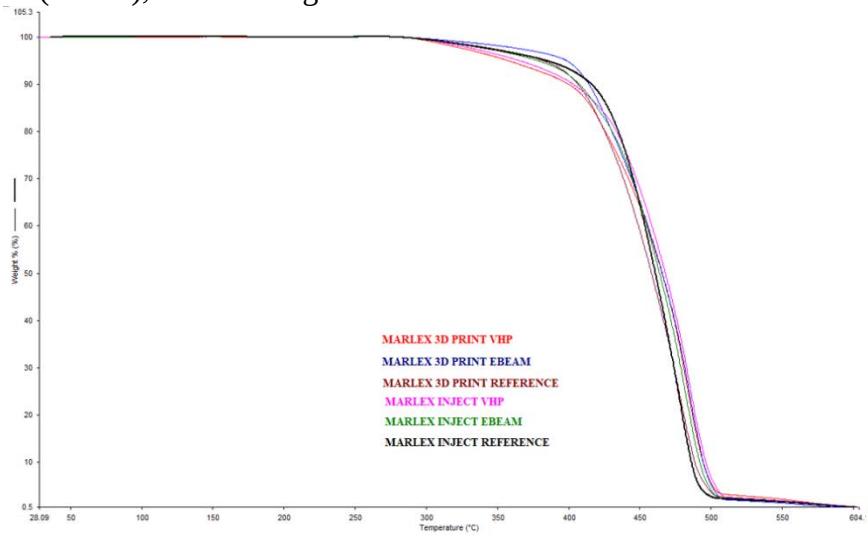

Figure 13: TGA curves of both 3D printed and injection moulded Marlex samples

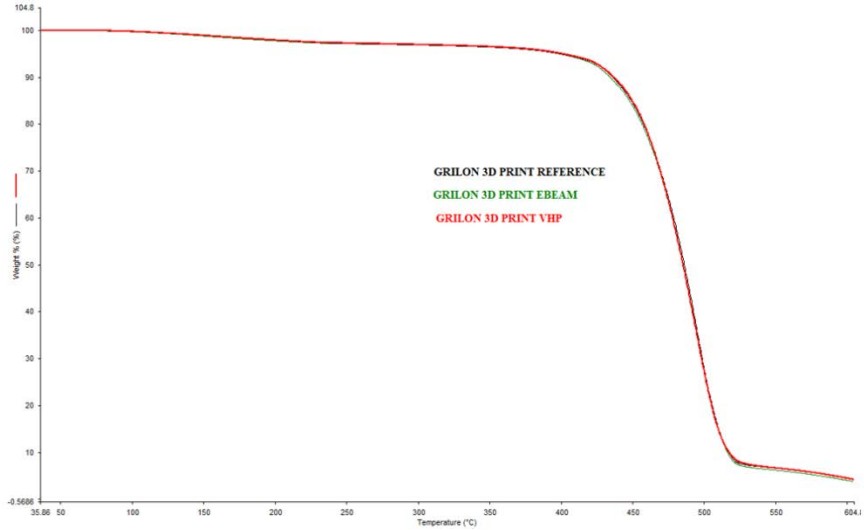

Figure 14: TGA curve of Grilon samples

Morphology

No noticeable change (i.e. cracks) was found on the surface of reference, VHP or E-beam treated samples, according to the SEM images, shown in figure 15.

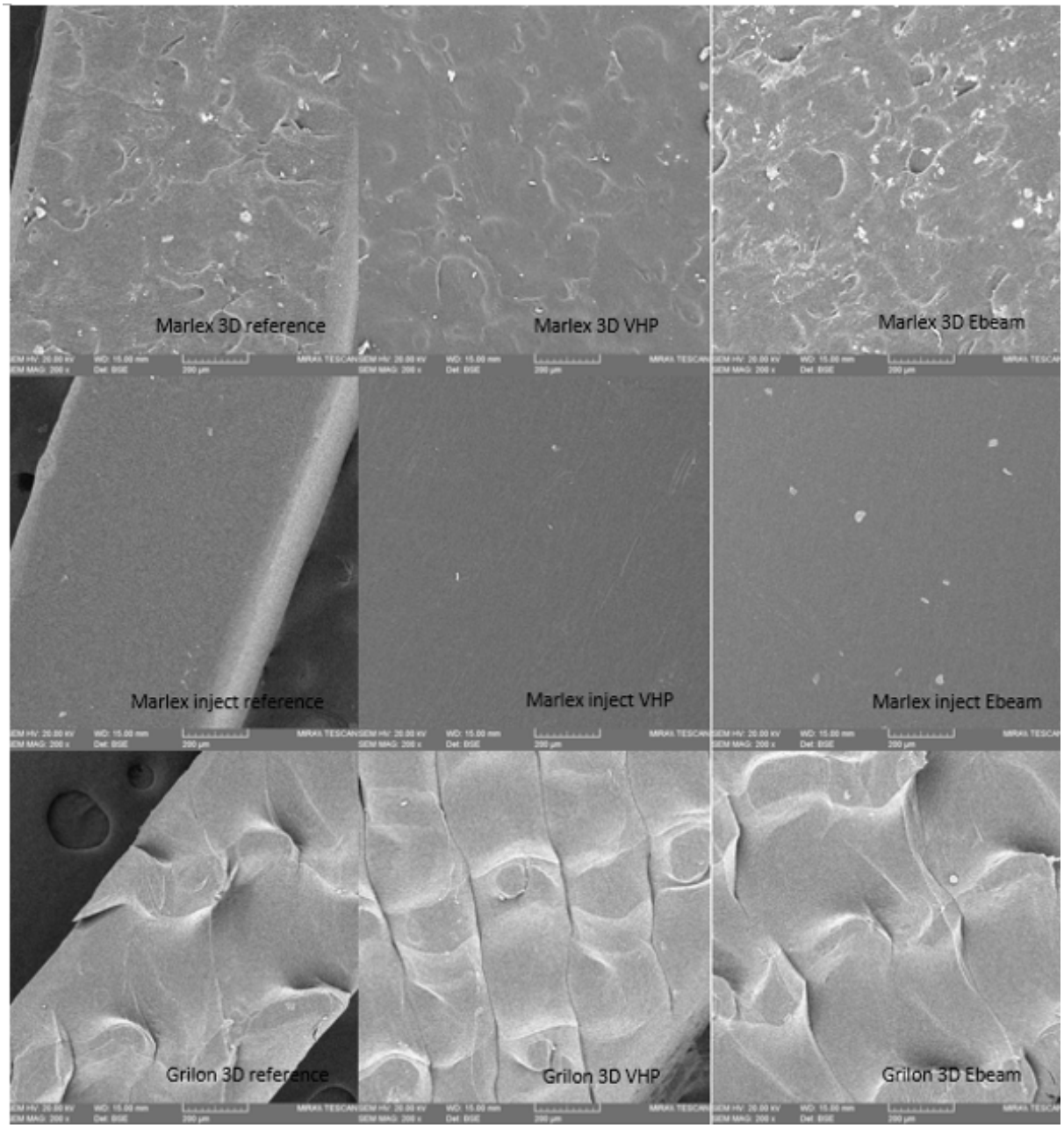

Figure 15: SEM images of 3D printed and injection moulded Marlex samples and 3D printed Grilon samples

Mechanical testing

Figure 16 illustrated the tensile test results of 3D printed and injection moulded Marlex samples. It clearly showed that the injection moulded Marlex samples have higher Young's modulus than the 3D printed Marlex samples, but with much lower percentage strain. VHP and E-beam processes did not cause significant change in Young's modulus (E) of 3D printed Marlex (309 ± 73 MPa, $p = 0.996$), injection moulded Marlex (385 ± 35 MPa, $p = 0.998$) or 3D printed Grilon samples (286 ± 96 MPa, $p = 0.699$). Similarly, VHP and E-beam did not cause significant change in their elongations either, with a percentage strain at maximum of 28 ± 1.8, 18.4 ± 1.7 and 375 ± 34 respectively ($p = 1$ for all comparison).

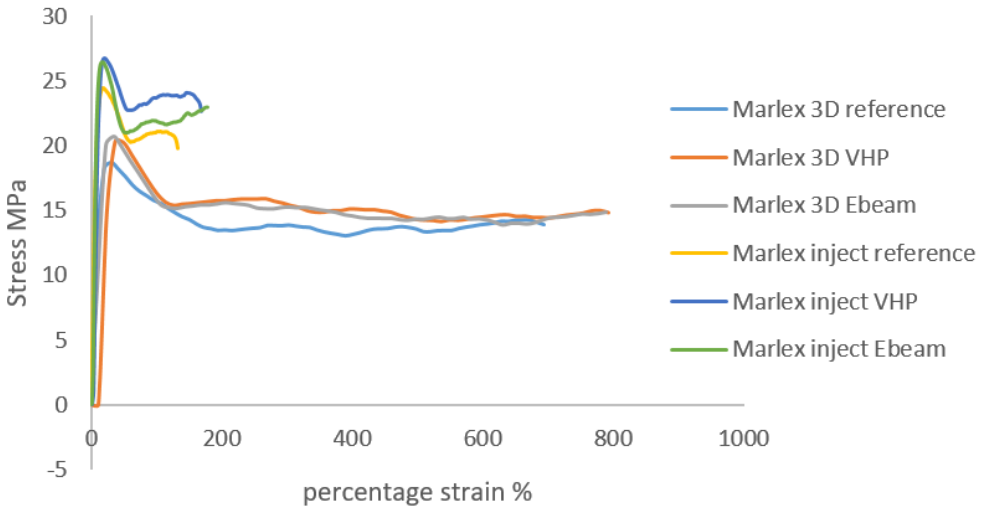

Figure 16: Tensile test results of Marlex samples

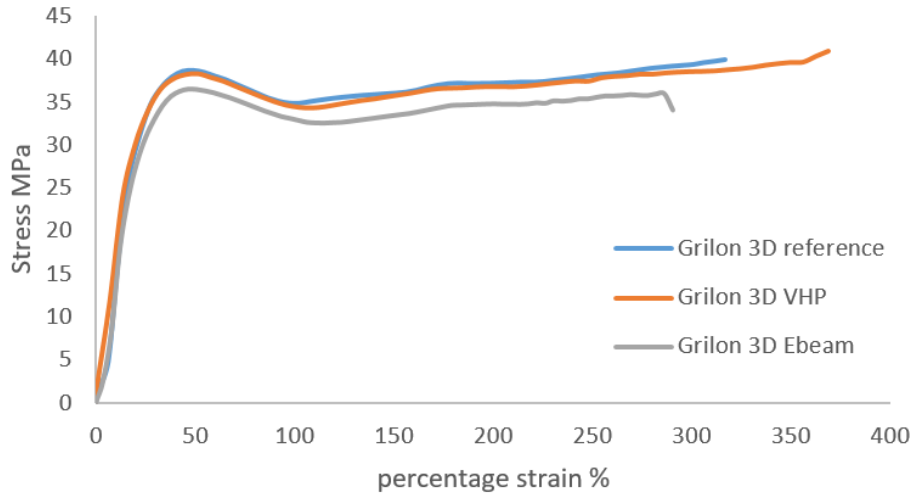

Figure 17: Tensile test results of Grilon samples

DISCUSSION

Oxidation occurred to all the samples after VHP and E-beam sterilization treatments, because all the samples turned yellow post sterilization. The free radicals produced by sterilization reacted with the oxygen diffusing through the material and caused bleaching of the radical based colour centres [20]. These free radicals were also responsible for the increasing hydrophilicity of the material, due to the formation of hydrophilic groups on the material surface by the radicals [11, 19]. In some cases, the material became opaque as a consequence of sterilization, but most treated materials changed colour to yellow or brown [9, 10]. In this study, E-beam treated samples appeared yellower than VHP treated samples, which may indicate that the E-beam process resulted in more severe oxidation than VHP process.

This can also be proved by FTIR results, where corresponding peaks for oxidation in the range of 3500 and 3100 cm^{-1} [23] were found in E-beam treated Marlex samples, but not in VHP treated Marlex samples. FTIR results also revealed that the sterilization processes resulted in crosslinking. The alkyl and allyl radicals are the predominant free radicals in polyethylene, which are able to bridge two long molecular chains by forming C - C intermolecular bonds or cross-linking that enhance the inter-chain interaction. The cross-linking mechanism of polyethylene involves two main stages. The first stage is the breakdown of the C-H bond on the polyethylene chains to produce hydrogen gas. The second stage is the free radicals react and join together to form cross-linking network [24]. Because some of the peaks related to

crosslinking appeared in the E-beam treated 3D printed Marlex samples but not in the E-beam treated injection moulded Marlex samples, it might indicate that the injection moulded samples were more stable than 3D printed samples upon E-beam sterilization process.

The results from DSC also supported that injection moulded samples were more stable than 3D printed samples upon sterilization processes. The E-beam treatment did not influence the percentage of crystallinity of injection moulded samples, but increased that of 3D printed samples dramatically. This can be attributed to the different structures due to the different manufacturing processes. Injection moulded samples have very tight structure due to the high pressure during the manufacturing process, while 3D printed samples are loosely packed with melt droplets. Therefore, there are more voids in 3D printed samples than injection moulded samples, and the voids allow more intermolecular crosslinking occur upon sterilization processes. The heavily cross-linked polymer chains in 3D printed samples hindered the mobility of the chains, resulting in the increase in the percentage of crystallinity [12, 13, 14, 15]. Compared to 3D printed Marlex samples, 3D printed Grilon samples did not display a dramatic increase in the percentage of crystallinity. The explanation would be that polyamide 6 tends to be stable upon sterilization methods within the limited cycles of sterilization processes [12,15].

Crosslinking after sterilization was also detected by rehometry and DMTA, where the viscosity, storage modulus and loss modulus increased after both VHP and E-beam processes. Viscosity refers to the resistance of the molten polymer to flow; the storage modulus and loss modulus are energy stored and energy dissipated in the material, when a deformation has been imposed. Crosslinking caused extra bonding between polymer chains, resulting in a reduction of molecular chains mobility in the interfacial region, hence causing interfacial stiffness which consequently increased the viscosity and improved the storage modulus of the material [29]. Yakacki *et al*. also mentioned that crosslinking of the shape memory polymers after gamma irradiation hindered the segmental motion of the polymer chains and resulted in the increase in rubbery modulus of the material [23]. This thermal properties study also revealed that E-beam treatment resulted in higher viscosity, storage modulus and loss modulus than VHP process, which indicated that E-beam process leads to more severe crosslinking effect than VHP treatment.

Despite the oxidation and crosslinking caused by VHP and E-beam treatments, the bulk properties of the samples were not affected, including thermal stability, mechanical properties and surface structure. The explanations are: 1) VHP sterilization process usually cause hydrolytic degradation of the samples, since Marlex and Grilon samples did not absorb moistures during VHP process, the hydrolytic degradation did not occur. It was reported that the molecular weight of polylactic acid (PLA) reduced significantly due to hydrolytic degradation when exposed to VHP treatment, because PLA is hygroscopic [30]; 2) The E-beam dosage of 30 kGy was not high enough to alternate the bulk properties. With a radiation dosage from 100 to 150 kGy, the thermal degradation of HDPE occured [31], small cracks were clearly observed on the surface of HDPE, the tensile strength and elongation at break of HDPE were increased due to crosslinking [13]. A rougher (flaky/scaly) surface of LDPE subsequent to E-beam irradiation at 400 kGy due to oxidative degradation was reported [22]. When the radiation dosage up to 500 kGy, the tensile strength and elongation at break of HDPE reduced significantly due to chain scission [13]. While polyamide 6 was reported not affected with single low radiation dosage, but the hardness, tensile strength, flexural strength and impact resistance of polyamide 6 were improved with the E-beam radiation up to 600 kGy, due to the increased cross-linking caused by radiation [32]. However, high irradiation dosage is not recommonded for sterilization purpose, and in general 25 kGy is a typical dose commonly employed to destroy the microbial load [7].

The tensile test results also revealed that the injection moulded Marlex samples had higher Young's modulus than the 3D printed Marlex samples, but had much lower percentage strain. The weaker mechanical properties of 3D printed objects compared to injection moulded objects can be explained by the layering manufacturing method of the 3D printing technology. The adhesion between layers or polymer strands plays a critical role in the mechanical properties of the 3D printed objects. Shaffer et al. reported that by improving the adhesion between polymer strands the chemical resistance and toughness of the 3D printed objected can be significantly improved [33]. In addition, the injection moulded Marlex samples had higher degree of crystallinity than 3D printed Marlex samples detected by DSC. The polymer chains of the injection moulded Marlex samples were pushed into highly organized structure with high pressure and cooled down quickly to form the shape, which results in high crystallinity, high mechanical strength, but low elongation. While the polymer chains of the 3D printed Marlex samples can move freely and cooled down slowly at room temperature, which results in relatively low crystallinity, low mechanical strength, but high elongation. This structure difference between injection moulded and 3D printed samples determined the different responds to VHP and E-beam processes as discussed above.

CONCLUSION

With the objective to investigate the effects of VHP and E-beam terminal sterilization processes on the 3D printed objects, this research studied the physical, chemical and thermal properties of 3D printed and injection moulded Marlex, and 3D printed Grilon samples upon VHP and E-beam terminal sterilization processes. The main findings were:

1. Oxidation occurred after both VHP and E-beam sterilization. Evidences included the discoloration and increased wettability due to the free radicals on the surface.
2. Crosslinking was caused by both VHP and E-beam sterilization treatment, evidenced with free hydroxyl radicals and intermolecular carbon bonding detected by FTIR; increased viscosity, storage modulus and loss modulus due to crosslinking.
3. E-beam treatment caused more severe oxidation than VHP process. Because the E-beam process resulted in more severe discoloration than VHP process, and the oxidation corresponding peaks detected by FTIR in E-beam treated samples, but not in VHP treated samples.
4. E-beam treatment caused more severe crosslinking than VHP process. Since E-beam process resulted in higher increase in viscosity, storage modulus and loss modulus than VHP treatment studied by rheometry and DMTA.
5. The 3D printed samples were less stable than injection moulded samples upon sterilization processes. Because more crosslinking associated peaks were detected by FTIR in 3D printed samples than in injection moulded samples, and E-beam process caused more dramatic increase in the degree of crystallinity of 3D printed samples than injection moulded samples.
6. Since the 3D printed objects were less stable than traditional manufactured objects, there may be a need to consider a reduction of sterilization parameters, especially for E-beam process, provided sterility assurance achieved.
7. Compared to 3D printed samples, the injection moulded samples exhibited higher tensile strength, higher degree of crystallinity, lower ductility, and higher thermal stability due to the tightly packed structures caused by injection moulding.
8. All the samples displayed a relatively good resistance to single cycle of VHP and E-beam process, evidenced with unaffected tensile properties, thermal stability and surface structure of all the samples.

DISCLOSURES

The authors declare that there is no conflict of interests regarding the publication of this article, this manuscript has not been published elsewhere and it has not been submitted simultaneously

for publication elsewhere. Martin Neff is an employee of ARBURG and Brian McEvoy is an employee of STERIS.

ACKNOWLEDGEMENTS

This publication has emanated from research conducted with the financial support of Athlone Institute of Technology under the Presidents Seed Fund, Enterprise Ireland funding under the Technology Gateway program, grant number TG-2017-0114 and Science Foundation Ireland (SFI) under Grant Number 16/RC/3918.

REFERENCES

[1] A. Reichental, How 3D printing is revolutionizing healthcare as we know it, TechCrunch. (2018). https://techcrunch.com/2018/04/05/bioprinted-organs-skin-and-drugs-how-3d-printing-is-revolutionizing-healthcare-as-we-know-it/ (accessed July 18, 2019).

[2] N.P. Tipnis, D.J. Burgess, Sterilization of implantable polymer-based medical devices: A review, Int. J. Pharm. 544 (2018) 455–460. doi:10.1016/j.ijpharm.2017.12.003.

[3] J. Hayes, D. Kirf, M. Garvey, N. Rowan, Disinfection and toxicological assessments of pulsed UV and pulsed-plasma gas-discharge treated-water containing the waterborne protozoan enteroparasite Cryptosporidium parvum, J. Microbiol. Methods. 94 (2013) 325–337. doi:10.1016/j.mimet.2013.07.012.

[4] Gamma Industry Processing Alliance, International Irradiation Association, White paper: A Comparison of Gamma, E-beam, X-ray and Ethylene Oxide Technologies for the Industrial Sterilization of Medical Devices and Healthcare Products, 2017. www.gipalliance.net (accessed July 23, 2019).

[5] U.S. FOOD & DRUG ADMINISTRATION, FDA Innovation Challenge 2: Reduce Ethylene Oxide Emissions | FDA, (2019). https://www.fda.gov/medical-devices/general-hospital-devices-and-supplies/fda-innovation-challenge-2-reduce-ethylene-oxide-emissions (accessed September 23, 2019).

[6] N.P. Tipnis, D.J. Burgess, Sterilization of implantable polymer-based medical devices: A review, Int. J. Pharm. 544 (2018) 455–460. doi:10.1016/j.ijpharm.2017.12.003.

[7] S. Govindaraj, S.M. Muthuraman, Systematic Review on Sterilization Methods of Implants and Medical Devices, Int. J. ChemTech Res. 8 (2015) 897–911. https://www.researchgate.net/publication/278242593.

[8] B. McEvoy, N.J. Rowan, Terminal sterilization of medical devices using vaporized hydrogen peroxide: a review of current methods and emerging opportunities, J. Appl. Microbiol. (2019) jam.14412. doi:10.1111/jam.14412.

[9] I. V. Puhova, A. V. Kazakov, K. V. Rubtsov, A. V. Medovnik, I. Kurzina, Modification of Polymer Materials by Electron Beam Treatment, Key Eng. Mater. 670 (2015) 118–125. doi:10.4028/www.scientific.net/kem.670.118.

[10] M. Sudol, K. Czaja, J. Cybo, P. Duda, Effect of electron-beam irradiation on structure of ultra high molecular weight polyethylene used in medical implants, Polimery/Polymers. 49 (2004) 841–844.

[11] K.J. Hemmerich, Polymer Materials Selection for Radiation-Sterilized Products | MDDI Online, Materials (Basel). (2000). https://www.mddionline.com/polymer-materials-selection-radiation-sterilized-products (accessed July 23, 2019).

[12] D.W. Plester, Effects of radiation sterilization on plastics, Steriliz. Technol. (1973) 151. https://inis.iaea.org/search/search.aspx?orig_q=RN:5109617.

[13] E.R. Elsharkawy, E.M. Hegazi, A.A.A. El-megeed, Effect of Gamma Irradiation on the Structural and Properties of High Density Polyethylene (HDPE), Int. J. Mater. Chem. Phys. 1 (2015) 384–387.

[14] V.R. Sastri, Engineering Thermoplastics: Acrylics, Polycarbonates, Polyurethanes, Polyacetals, Polyesters, and Polyamides, in: Plast. Med. Devices, William Andrew

Publishing, 2010: pp. 121–173. doi:10.1016/B978-0-8155-2027-6.10007-8.
[15] G. Kubyshkina, B. Zupančič, M. Štukelj, D. Grošelj, L. Marion, I. Emri, Sterilization effect on structure, thermal and time-dependent properties of polyamides, J. Biomater. Nanobiotechnol. 2 (2011) 361–368. doi:10.1007/978-1-4614-0213-8_3.
[16] E. Shaheen, A. Alhelwani, E. Van De Casteele, C. Politis, R. Jacobs, Evaluation of Dimensional Changes of 3D Printed Models After Sterilization: A Pilot Study, Open Dent. J. 12 (2018) 72–79. doi:10.2174/1874210601812010072.
[17] A.T. Miller, D.L. Safranski, K.E. Smith, D.G. Sycks, R.E. Guldberg, K. Gall, Fatigue of injection molded and 3D printed polycarbonate urethane in solution, Polymer (Guildf). 108 (2017) 121–134. doi:10.1016/J.POLYMER.2016.11.055.
[18] M. Dawoud, I. Taha, S.J. Ebeid, Mechanical behaviour of ABS: An experimental study using FDM and injection moulding techniques, J. Manuf. Process. 21 (2016) 39–45. doi:10.1016/J.JMAPRO.2015.11.002.
[19] M. Neff, O. Kessling, Layered Functional Parts on an Industrial Scale, Kunststoffe Int. (2014). www.kunststoffe-international.com (accessed May 9, 2019).
[20] R.L. Clough, K.T. Gillen, G.M. Malone, J.S. Wallace, Color formation in irradiated polymers, in: Radiat. Phys. Chem., Pergamon, 1996: pp. 583–594. doi:10.1016/0969-806X(96)00075-8.
[21] A.M. Abdul-Kader, A. Turos, R.M. Radwan, A.M. Kelany, Surface free energy of ultra-high molecular weight polyethylene modified by electron and gamma irradiation, Appl. Surf. Sci. 255 (2009) 7786–7790. doi:10.1016/j.apsusc.2009.04.176.
[22] K.A. Murray, J.E. Kennedy, B. Mcevoy, O. Vrain, D. Ryan, R. Cowman, C.L. Higginbothama, Characterisation of the Surface and Structural Properties of Gamma Ray and Electron Beam Irradiated Low Density Polyethylene, Int. J. Mater. Sci. 3 (2013) 1–8.
[23] C.M. Yakacki, M.B. Lyons, B. Rech, K. Gall, R. Shandas, Cytotoxicity and thermomechanical behavior of biomedical shape-memory polymer networks post-sterilization, Biomed. Mater. 3 (2008) 015010. doi:10.1088/1748-6041/3/1/015010.
[24] S.-T. Bee, W.-K. Wong, A.R. Rahmat, T.-T. Tee, C.T. Ratnam, J.-X. Lee, L.T. Sin, Effects of electron beam irradiation on the structural properties of polylactic acid/polyethylene blends, Nucl. Instruments Methods Phys. Res. Sect. B Beam Interact. with Mater. Atoms. 334 (2014) 18–27. doi:10.1016/j.nimb.2014.04.024.
[25] F.G.D. Ferreira, M.A.G. de A. Lima, Y.M.B. de Almeida, G.M. Vinhas, Effect of the radiolitic sterilization in polyethylene/starch blends, Quim. Nova. 31 (2008) 1043–1047. doi:10.1590/S0100-40422008000500018.
[26] S. Luo, A.N. Netravali, Effect of 60Co γ-radiation on the properties of poly(hydroxybutyrate-co-hydroxyvalerate), J. Appl. Polym. Sci. 73 (1999) 1059–1067. doi:10.1002/(SICI)1097-4628(19990808)73:6<1059::AID-APP25>3.0.CO;2-Q.
[27] S. Fuchs, T. Schmidt, S. Haftka, J. Jerosch, [Changes in crystallinity by sterilization and processing of ultrahigh molecular polyethylene used in endoprosthetics]., Unfallchirurg. 101 (1998) 382–7. http://www.ncbi.nlm.nih.gov/pubmed/9629051 (accessed May 1, 2019).
[28] O.Y. Alothman, H. Fouad, S.M. Al-Zahrani, A. Eshra, M.F. Al Rez, S.G. Ansari, Thermal, creep-recovery and viscoelastic behavior of high density polyethylene/hydroxyapatite nano particles for bone substitutes: Effects of gamma radiation, Biomed. Eng. Online. 13 (2014) 125. doi:10.1186/1475-925X-13-125.
[29] N.D. Zaharri, Effect of peroxide cross-linking on viscoelastic behaviour and thermal properties of zeolite filled ethylene vinyl acetate composite, in: Compos. Adv. Manuf. Characterisation, 2016: pp. 177–186. doi:10.2495/978-1-78466-167-0/018.
[30] D. Bhatnagar, K. Dube, V.B. Damodaran, G. Subramanian, K. Aston, F. Halperin, M.

Mao, K. Pricer, N.S. Murthy, J. Kohn, Effects of Terminal Sterilization on PEG-Based Bioresorbable Polymers Used in Biomedical Applications, Macromol. Mater. Eng. 301 (2016) 1211–1224. doi:10.1002/mame.201600133.

[31] S.O. Han, D.W. Lee, O.H. Han, Thermal degradation of crosslinked high density polyethylene, Polym. Degrad. Stab. 63 (1999) 237–243. doi:10.1016/S0141-3910(98)00098-6.

[32] N.K. Pramanik, R.S. Haldar, Y.K. Bhardwaj, S. Sabharwal, U.K. Niyogi, R.K. Khandal, Radiation processing of Nylon 6 by e-beam for improved properties and performance, Radiat. Phys. Chem. 78 (2009) 199–205. doi:10.1016/j.radphyschem.2008.11.004.

[33] S. Shaffer, K. Yang, J. Vargas, M.A. Di Prima, W. Voit, On reducing anisotropy in 3D printed polymers via ionizing radiation, Polymer (Guildf). 55 (2014) 5969–5979. doi:10.1016/J.POLYMER.2014.07.054.